

In vivo Raman Measurements of Human Skin

Introduction

Confocal Raman spectroscopy is beginning to be recognized as a high potential technique for the non invasive study of biological tissues and human skin under *in vivo* conditions. Raman spectroscopy can be applied to obtain information regarding the molecular composition of the skin down to several hundred micrometers below the skin surface. The stratum corneum is the skin's outermost layer and the main protective barrier against water loss, microorganisms and toxic agents of the epidermis. Non-invasive confocal Raman spectroscopy could give some insight of structure and mechanisms governing the behaviour of this layer. Moreover, in-depth measurements allow the determination of relative concentration modifications of the major constituents (water, urea, proteins...) in the thickness of the epidermis. Such information is of major interest for the development of *in vivo* diagnosis of skin diseases and the improvement of transdermal drug administration.

We present here in depth spectra of the epidermis from which we can obtain information regarding its composition. Surface point measurements and in-depth profiles were also performed on "hydrated" and "non hydrated" fingertip skin to monitor possible variations of water content versus depth.

To undertake *in vivo* Raman analysis of human skin one has to cope with some specific behaviour of this "living" sample which are crucial when wanting to record an optimum spectrum. Indeed, body movements and heart beat may affect the laser focal point. Consequently, using a classical upright configuration -in which the sample lies beyond the microscope- to examine the skin surface of a finger is not an optimum set-up. That's why the skin measurements on the tip of the index finger reported here were recorded using an inverted configuration which definitely improves the ease of sampling.

Analyses have been carried out with different laser excitations in the red (633nm) and near infrared (785nm, 830nm) to avoid the possible fluorescence of the tissues and

determine the respective advantages of such wavelengths.

Experimental and technical aspects

1. Sample

All measurements were made on the index fingertips of two volunteers (both female, 27 years old).

In order to induce variations in the water content of the skin, some experiments have been carried out on a same person on one "non-hydrated" finger and on the other finger recently "hydrated" with a moisturizing cream.

2. Experimental Set-Up

The **LabRam INV** is an integrated and compact Raman system equipped with an inverted confocal microscope (i.e. the sample lies above the microscope) directly coupled to the spectrograph.

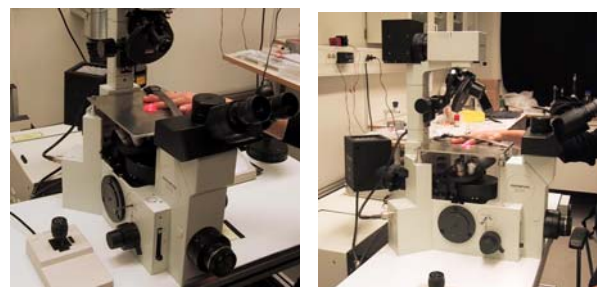


Figure 1. Position of the index finger on the microscope stage during analysis.

The index fingertip was examined on the microscope stage of the inverted microscope (Fig.1). A metal plate was firmly screwed at the position traditionally assigned to the motorized stage. A 25 mm diameter hole was drilled at the middle of the plate for sampling.

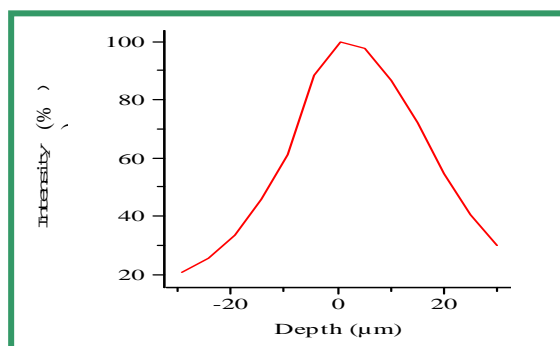
This hole could be filled either with a second round metal piece with a 1 mm hole in the middle or a 2mm-thick quartz window. In both cases, the part of the hand investigated can lie in a flat and stable way during the experiment. To prevent any hand movement, a strap and

some tape were used to ensure the fingers remain still. We checked that the measurement is repeatable by recording five successive spectra of the CH/OH region on the surface of the sample. This showed a good focus stability with band area fluctuation of less than 5%.

3. Measurement Conditions

Two different objectives were used depending on the wavelength range: 20X LWD NIR (N.A=0.40) and 50X LWD visible (N.A=0.55). The laser power available at the sampling point is around 5-10 mW, spectra were recorded at the three wavelengths 633, 785 and 830 nm in a few tenth of seconds.

Before undertaking surface and in-depth profile measurements, we determined the approximate depth of focus of the objective used which is directly linked with the volume from which Raman signal is collected. For all measurements, the confocal hole was opened at either 200 or 400 μm to find the best compromise between axial resolution and signal intensity due to the limited laser power at the sampling point. The depth of focus was roughly estimated for such a confocal hole and for both objectives (50X LWD visible and 20X LWD NIR) and the results are presented below. For the evaluation of the depth of focus, a silicon sample was moved through the laser focus and the signal going through the confocal pinhole was measured. The axial resolution is inferred from the width of the response curve at 50% of the maximum signal (Full Width at High Maximum). The derived axial resolutions are shown below.



Wavelength	Confocal hole	Objective	FWHM
633 nm	200	20X	25-30 μm
633 nm	200	50X	6-8 μm
785-830 nm	200	20X	25-30 μm
785-830 nm	400	20X	40-45 μm

Figure 2: Top: example of the intensity response curve of the Silicon band.(521 cm^{-1}) for the determination of the depth of focus. Bottom: FWHM value depending on system parameters.

Results

1. Choice of the excitation wavelength: spectra recorded at 633nm, 785nm and 830nm

We recorded the Raman spectra of the surface skin at 633nm, 785nm and 830nm which are shown Fig.3a. The CDD response is however reduced in the high frequencies domain at 785nm and even limited to 2200 cm^{-1} at 830nm which can be rather limiting when wishing to observe the OH, NH and CH stretching modes lying around 2800 cm^{-1} up to 3500 cm^{-1} . It is then necessary to select InGaAs detectors optimized for the NIR region. In this application, the use of the readily implemented 633nm laser excitation for skin analysis is possible without observing any tissue autofluorescence. However, for other in vivo applications (i.e. study of internal organs such as liver, brain, muscles...) and the investigated skin which has undergone cosmetic pre-treatments (hydration for example), it is sometimes preferable to use Near InfraRed excitations to avoid interference of fluorescence emission. Moreover, powerful lasers focused on micrometric surfaces lead to increases in most tissue temperature⁴. As most tissues exhibit a minimum absorption of light in the NIR domain⁵, using excitation wavelength in this domain will minimize the risks of sample heating and/or photochemical interactions.

2. The fingerprint region

The Figure 3b shows the Raman spectrum of the surface of the skin in which Raman signature of the numerous constituents of the epidermis is well defined. Two typical Raman features of the collagen are identified in the spectrum at 855 cm^{-1} and 936 cm^{-1} .

Other Raman bands can be assigned to the family of Protein or to the family of Lipids constituting the tissue (see Tab. 1).

The 1655 cm^{-1} peak is attributed to protein keratin (80% of the dry weight of the stratum corneum). Moreover, the fingerprint region

gives access to the Raman signature of major amino acids and derivatives constituents of the human natural moisturizing factors. A detailed study of this fingerprint region provides information on the molecular relative composition and conformation of some of the molecular species.

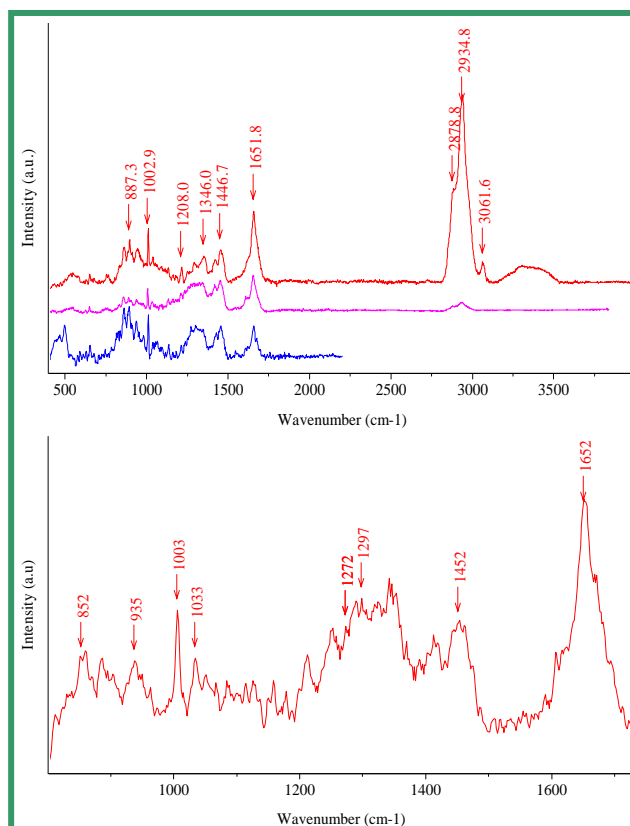


Figure 3. (a) Raman spectra of the surface of the fingertip of the index finger recorded at 633nm,785nm, 830nm .(b) detail of the fingerprint region recorded at 633nm.

3. Fingerprint: In-depth measurements

Figure 4 shows a series of spectra acquired from the surface to 240 μm inside the skin with a 40 μm step. This large step was chosen due to the large depth of field of the objective used (here obj. 20x, 633nm).

We still obtain exploitable spectra down to a 240 μm depth in the skin. The shoulder located at 1616 cm^{-1} seems to vanish when penetrating deeper into the skin. The band at 1412 cm^{-1} also decreases when probing deeper. These subtle changes are also observed by Puppels *et al.*¹⁻³. This observation has been reproduced in a similar experiment performed at 785nm.

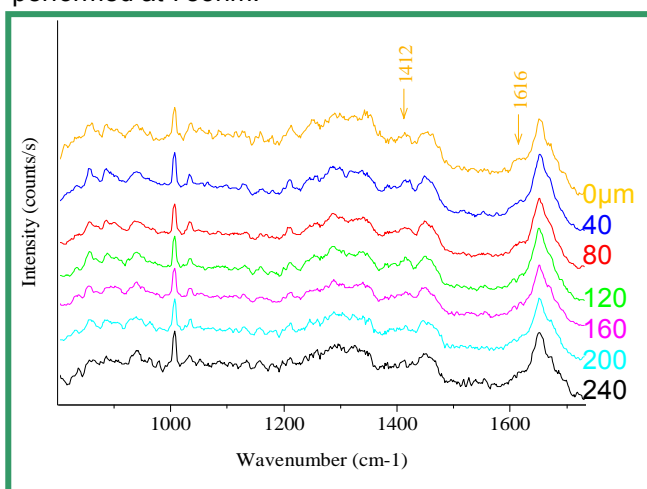


Figure 4. Spectra of the fingerprint region measured at different depths (μm). All spectra have been normalized with respect to the 1000 cm^{-1} band and artificially translated for a better comparison

Peak Position (cm^{-1})	Protein Assignments	Lipid Assignments	Others
1745		V(C=O)	
1655	V(C=O)Amide I		
1445	$\delta(\text{CH}_2)$, $\delta(\text{CH}_3)$ δ	$\delta(\text{CH}_2)$ scissoring	
1301		$\delta(\text{CH}_2)$ twisting, wagging	
1269	v(CN), $\delta(\text{NH})$ Amide III		
1080		v(CC)skeletal	v(CC), $v_s(\text{PO}_2)$
1030		v(CC) skeletal	Nucleic acids
1002	v(CC) Phenyl ring		
938	v(CC) praline, valine		
855	$\delta(\text{CCH})$ aromatic, olefinic		polysaccharide
822	$\delta(\text{CCH})$ aliphatic		

Table 1: Summary of major vibrational bands identified in skin: v, stretching mode; v_s , symmetric stretch; δ , bending mode.

4. $\nu(\text{CH})/\nu(\text{OH})/\nu(\text{NH})$ region: Comparison of water concentration in hydrated and non-hydrated skins.

In-depth spectra are recorded each 30 μm from the surface of the index fingertip down to 300 μm in the skin. For a better comparison of the spectra, those are normalized with respect to the CH band area integrated in the range [2910-2965] cm^{-1} .

In the range [3200-3600] cm^{-1} , the complex broad band (see Fig. 3a, spectrum at 633nm), is constituted of the $\nu(\text{OH})$ broad band and of the $\nu(\text{NH})$ thinner band located around 3300 cm^{-1} .

The evolution of the water content in tissue can be determined by calculating the area below a part of the complex broad band in the range [3350-3550] cm^{-1} of the normalized spectra (see Puppels *et al.*¹⁻³)

In the case of the non hydrated skin, the 3D representation of the Figure 5a clearly shows an increase of the intensity the $\nu(\text{OH})$ - $\nu(\text{NH})$ complex band and of the weak band located at 3060 cm^{-1} (assigned to the aromatic CH stretching mode) when depth increases. Figure 5b also points out the relative increase of water content as depth increase.

In the case of the hydrated index finger, Figure 6a clearly shows a parallel increase of intensity of the $\nu(\text{OH})$ - $\nu(\text{NH})$ complex band and of the peak located at 3060 cm^{-1} . Figure 6b highlights that after hydration the water content is higher at the fingertip surface and 270 μm deep. By comparison with the profile recorded before the hydration, this measurement demonstrates the effect of the moisturizing cream on skin surface.

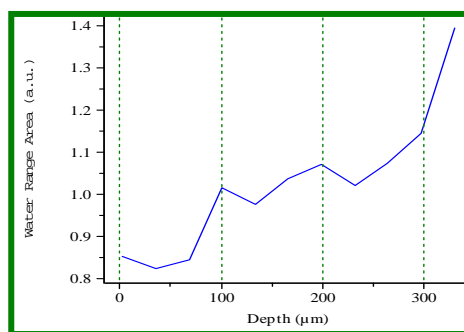


Figure 5 : **Non hydrated skin** (a) 3D view of the spectra of the CH/OH region recorded at different depths within the non hydrated skin. (b) In-depth profile of the relative evolution of the $\nu(\text{OH})$ band area [3350-3550] cm^{-1} .

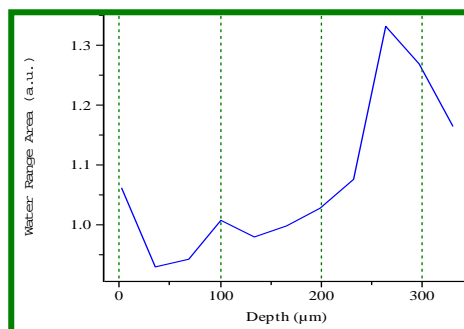
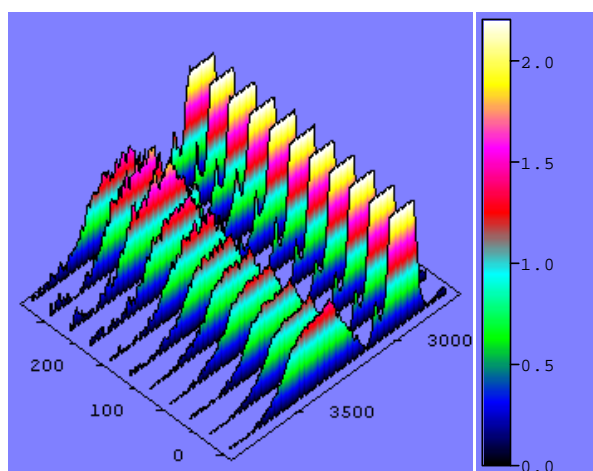
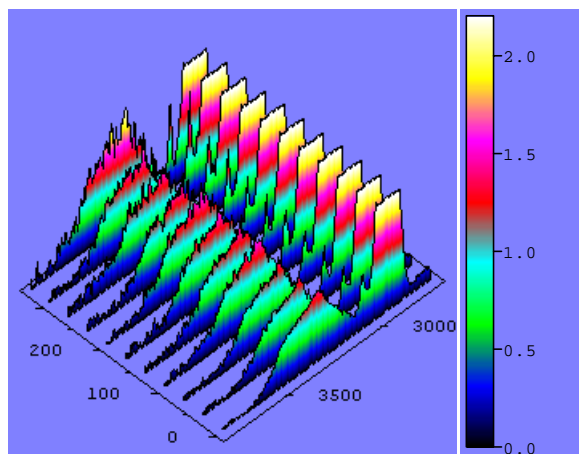


Figure 6 : **Hydrated skin** (a) 3D view of the spectra of the CH/OH region recorded at different depths within the hydrated skin. (b) In-depth profile of the relative evolution of the $\nu(\text{OH})$ band area [3350-3550] cm^{-1} .





Conclusion

Thanks to confocal Raman spectroscopy we have been able to investigate *in vivo* the epidermis chemical composition in its thickness. In depth measurements allowed us to observe modifications of the relative concentration of some components (water, proteins) depending on the depth in the skin and on its state of hydration.

The use of larger numerical aperture objectives would be helpful to emphasize the in-depth variations because of the possible gain in axial resolution and therefore in-depth discrimination. Indeed, the operator could then probe in depth with a smaller step size.

As a possible gain on the above measurements, the use of more powerful commercially available NIR diode lasers would yield up to ten times more laser power at the sample (60-80 mW) and would result in a tremendous improvement in terms of signal collection and integration time.

Acknowledgement: We are grateful to the Institute of Analytical and Marine Chemistry, University of Chalmers, Göteborg, Sweden as they welcomed us to carry out these measurements on their LabRAM INV.

References

1. "In Vitro and In Vivo Raman Spectroscopy of Human skin", P.J. Caspers, G.W Lucassen, R. Wolthuis, H.A. Bruining, G.J. Puppels, *Biospectroscopy*, 4, S31-S39, 1998.
2. "In Vivo Confocal Raman Microspectroscopy of the skin : Noninvasive determination of molecular concentration profiles " , P.J. Caspers, G.W Lucassen, Elizabeth A. Carter, R. Wolthuis, H.A. Bruining, G.J. Puppels, 2001
3. "Automated depth scanning confocal Raman Microspectrometer for rapid in-vivo determination of water concentration profiles in human skin", P.J. Caspers, G.W Lucassen, H.A. Bruining, G.J. Puppels, 2000
4. Handbook of Raman Spectroscopy. Practical spectroscopy series volume 28. Ed. Ian R. Lewis and Howell G. M. Edwards, pp549-574.
5. Handbook of Vibrational Spectroscopy, vol.5, Ed. J.M. Chalmers and P.R. Griffiths, Wiley, pp3362-3375.